Molecular Crystals and Liquid Crystals Science and Technology. Section A. Molecular Crystals and Liquid Crystals

Publication details, including instructions for authors and subscription information:
http://www.tandfonline.com/loi/gmcl19

Development of an All-Atom Force Field for the Simulation of Liquid Crystal Molecules in Condensed Phases (LCFF)

Melanie J. Cook [a] & Mark R. Wilson [a]

[a] Department of Chemistry, University of Durham, South Road, Durham, DH1 3LE, UK

Version of record first published: 24 Sep 2006

To cite this article: Melanie J. Cook & Mark R. Wilson (2001): Development of an All-Atom Force Field for the Simulation of Liquid Crystal Molecules in Condensed Phases (LCFF), Molecular Crystals and Liquid Crystals Science and Technology. Section A. Molecular Crystals and Liquid Crystals, 357:1, 149-165

To link to this article: http://dx.doi.org/10.1080/10587250108028250

Mol. Cryst. Liq. Cryst., Vol. 357, pp. 149-165
Reprints available directly from the publisher
Photocopying permitted by license only

Development of an *All-Atom* Force Field for the Simulation of Liquid Crystal Molecules in Condensed Phases (LCFF)

MELANIE J. COOK and MARK R. WILSON*

Department of Chemistry, University of Durham, South Road, Durham DH1 3LE, UK

(Received August 10, 2000; In final form October 9, 2000)

A set of intermolecular potential energy functions have been developed for use in computer simulations of mesogenic molecules in the isotropic and liquid crystalline phases. Primarily, the force field parameters have been developed for the mesogens GG5Cl and me5NF. Together, these molecules contain a number of important structural features present in many calamitic mesogens: including conjugated phenyl rings, lateral fluorination, an ester group, alkyl chains, terminal dipolar groups (chloro and cyano groups respectively). Where possible we have adopted data from the AMBER and OPLS-AA force fields to describe these systems, and have extended these force fields using a combination of high level quantum mechanical calculations and X-ray structural data. The potential functions obtained in this way are used to define a liquid crystal force field (LCFF) that can be extended easily to other mesogens containing different fragments. Validation of the LCFF was carried out by computing structural and thermodynamic data for the molecules me5NF, GG5Cl and the *mesogenic fragments* phenyl acetate and methyl benzoate using molecular dynamics simulations.

Keywords: liquid crystals; force field; molecular simulation; molecular dynamics; LCFF

1 INTRODUCTION

Computer modelling is becoming increasingly important as a tool to study the structure and dynamics of liquid crystal molecules and liquid crystal phases. One of the key modelling areas is that of *molecular modelling* where classical potential energy functions are used to describe both intra- and intermolecular interactions for any given system [1,2]. For example, there has recently been considerable progress in simulating bulk liquid crystal phases using either Monte Carlo or molecular dynamics simulation methods to sample intra- and intermolecular degrees of freedom [3–11]. At the heart of such calculations are molecular mechanics force fields that describe the total energy of the molecules as a sum

* Corresponding Author.

of the steric and nonbonded interactions present. Given the importance of these force fields, careful consideration should be made to the functional form used, and the parameters required in order to apply them to liquid crystal systems.

In standard force fields the molecule is considered as a collection of atoms joined together by elastic restoring forces. These forces are described by simple mathematical functions that characterize the distortion of each structural feature within the molecule: bond stretches, angle bends, torsional angle deformations and nonbonded interactions. Over the years considerable work has been undertaken in order to develop new potentials that accurately model intermolecular interactions. In the early days molecular modelling was influenced strongly by the desire to model biological systems. Consequently, much of the initial work was centered around developing accurate parameters focussed on biomolecules, particularly peptides and nuclei acids resulting in force fields such as CHARMM [12,13] and AMBER [14]. These force fields have now been extended to contain many new parameters which cover a wider range of organic molecules [15]. A different strand of force field development stems from the work of Allinger and co-workers with their development of the MM1 [16], MM2 [17], MM3 [18] and MM4 [19–23] force fields based on predicting the structures and conformational energies of isolated organic molecules. Most recently we have seen the development of Jorgensen's OPLS (Optimised Potentials for Liquid Simulations) all atom and united atom force fields [24–28]. The latter has already proved to be useful in bulk simulations of liquid crystal molecules [3–5].

The current paper considers the adaptation of the OPLS (all-atom) and AMBER force fields to typical liquid crystal molecules. In particular, we consider the derivation of a force field for the liquid crystal molecules me5NF and GG5Cl (figure 1) that, between them, contain common structural features present in many mesogens: conjugated phenyl rings, lateral fluorination, an ester group, alkyl chains, terminal dipolar groups (chloro and cyano groups respectively). We employ *ab initio* quantum mechanical studies of fragments of these molecules and X-ray structural data to derive force fields parameters, and we carry out state-of-the-art molecular dynamics simulations of the *fragment molecules* phenyl acetate and methyl benzoate in the bulk liquid to test the force field. The computed results are compared directly to experimental thermodynamic and structural data. The layout of this work is as follows. In section 2, we discuss the choice of functional form for our liquid crystal force field, in section 3 we determine force field parameters for this form and then use these in section 4 to simulate phenyl acetate, methyl benzoate, me5CF and GG5Cl in the bulk liquid phases. We summarise in section 5. Finally, we make use of the force fields derived in this work in the next paper in this issue [29] to study dipole correlation in the pretransitional region of the isotropic phase of me5NF and GG5Cl.

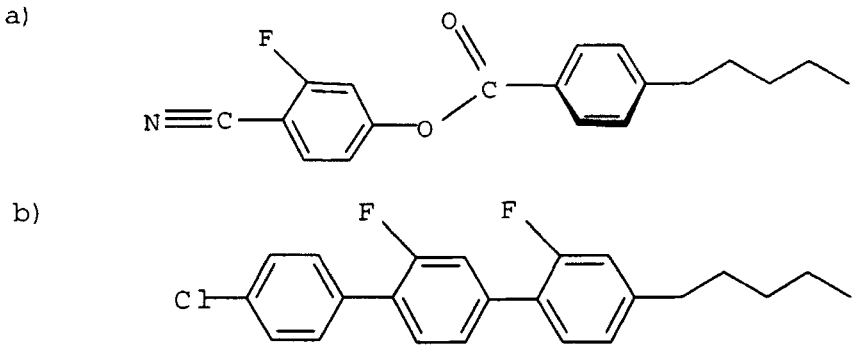

FIGURE 1 Structure of a) me5NF and b) GG5Cl

2 CHOICE OF FUNCTIONAL FORM FOR THE LIQUID CRYSTAL FORCE FIELD

A number of elements come into consideration when choosing a functional form for a liquid crystal force field. The most accurate single molecule force fields are currently the MM4 [19–23] and the Merck Molecular Force Field (MMFF94) [30–34]. Both these force fields use an exponential form for the repulsive part of the nonbonded interactions. While this is certainly more accurate than a $1/r^{12}$ form at short intermolecular separations, it is extremely expensive for bulk simulations of mesogens where thousands of nonbonded interactions must be computed in a single molecular dynamics step or in a Monte Carlo trial move. Consequently, in this work we have followed the OPLS and AMBER force fields and have adopted a Lennard-Jones 12:6 form to describe the nonbonded parameters. At the temperature and pressure ranges normally associated with mesophases (250–450 K, 1 atmosphere) we would expect the sampling of the high energy region of the repulsive part of the potential to be a relatively rare event. Moreover, in fluid states of matter, groups are constantly in motion, so modelling the closest approach of atoms to the highest level of accuracy is less important that it would be in (say) a crystal. Consequently, the choice of a $1/r^{12}$ repulsive term is the optimum one for liquid crystal work. We also note the importance of using *effective two-body potentials* to describe the nonbonded interactions. For reasons of computational expense, the use of *three body potentials* for mesogen simulation is currently out of the question. However, in a normal fluid we would expect a sizeable contribution to the nonbonded interactions to arise from *three*

body terms. For practical purposes these contributions must currently be consumed into the *two body terms*. Consequently, we expect the best *effective two body potentials* to be those that arise from fitting to the thermodynamic properties of real liquids, rather than those found by fitting to pair-interaction structures/energies in the gas phase. Jorgensen has taken this approach in designing the OPLS force field relying on Monte Carlo simulations of small molecules to allow fitting to liquid state properties to obtain the *two body* potentials. A recent comparison of MMFF94 and OPLS-AA [35] in simulating liquid butane, methanol, and N-methylacetamide testifies to the usefulness of this approach.

The other main difference between force fields is in the number and type of terms used to describe the intramolecular degrees of freedom. The MM4 and MMFF94 use more sophisticated potentials with many more terms (including cross-terms such as bend-stretch interactions) whereas many simpler force fields use a simple harmonic force field (as described below – see equation 1). In this work we have followed the AMBER approach and chosen a harmonic force field. In simulating bulk phases it is rarely necessary to describe bond lengths or angles to the same degree of accuracy as required in predicting the minimum energy of a molecule in the gas phase. Indeed it is often useful to fix bond lengths using the SHAKE method [36] in order to increase the time-step within a molecular dynamics simulation. Instead the main problem in simulating mesogens arises in determining good torsional potentials (see section 3). Rotation about bonds requires relatively small changes to the internal energy, but can lead to large changes in structure for rod-shaped molecules. Consequently, internal rotations are strongly coupled to molecular packing in a fluid [11,37] and hence have a major influence on transition temperatures.

The final key consideration in designing a LCFF is in choosing an *all atom* or a *united atom* form. The latter replaces hydrogens on attached carbons by single *united atom* potentials. This has large advantages in terms of savings in computer time and has been used in most previous liquid crystalline simulations [1]. However, recent work by the current authors on PCH5 indicates that hydrogens attached to carbons in a phenyl ring fulfil a vital role. Inclusion of partial charges on both the hydrogens and the carbons in an aromatic ring allows the ring quadrupole to be modelled and quadrupolar interactions have a significant influence on short range packing of mesogenic molecules [38]. We have therefore included hydrogens explicitly in the current work, particularly as we wish to use the force field to study dipole correlation in me5CN and GG5Cl. We note that Garcia *et al* [39] have recently described a hybrid force field for a group of liquid crystal molecules where phenyl hydrogens are included explicitly but aliphatic hydrogens are excluded. Their approach seems a useful compromise, between keeping vital interactions and minimising computer time.

Using the principles described above we write our LCFF force field in the AMBER/OPLS form

$$E_{\text{total}} = \sum_{\text{angle}} K_\theta(\theta - \theta_{eq})^2 + \sum_{\text{dihedral}} \left(\sum_{m=1}^{6} \frac{V_m}{2}[1 + \cos(m\phi - \delta_m)] \right) \sum_{i<j} \left(\frac{q_i \cdot q_j}{r_{ij}} + \frac{A_{ij}}{r_{ij}^{12}} - \frac{C_{ij}}{r_{ij}^{6}} \right) f_{ij}. \quad (1)$$

In equation 1, K_θ, V_m are force constants representing angle bending and torsional motion respectively; the nonbonded energy between atoms i and j at a distance r_{ij} are represented by a Coulomb plus Lennard-Jones potential, where A_{ij} and C_{ij} can be expressed in terms of the well depth and collision parameters, ε_{ij} and σ_{ij} respectively: $A_{ij} = 4\epsilon_{ij}\sigma_{ij}^{12}$, $C_{ij} = 4\epsilon_{ij}\sigma_{ij}^{6}$. ($f_{ij} = 0.5$ for 1,4 12:6 nonbonded terms, $f_{ij} = 0.125$ for 1,4 electrostatic terms and $f_{ij} = 1$ for all other nonbonded interactions.)

3 DETERMINATION OF FORCE FIELD PARAMETERS

For the molecules me5NF and GG5Cl we require the 10 atom types described in table I. As a starting point for the current work we have used the OPLS-AA all-atom force field of Jorgensen and co-workers [27,28,40] optimised to reproduce the correct densities and heats of vaporization for a series of small organic molecules. The merger of the OPLS-AA non bonded potential functions and the intramolecular AMBER force field parameters has already been considered [27,41] and we follow the convention used in these references whereby 1–4 Lennard-Jones interactions are scaled by a factor of 2 (compared to intermolecular interactions) and electrostatic interactions are scaled by a factor of 8. All of the nonbonded parameters used in the current work are summarised in table II. The partial charges of table II are significantly higher than those obtained from minimal basis set Mullikan charge distributions calculated from ab initio molecular orbital calculations. The latter give inadequate results when used to verify properties of pure liquids, and are unable to properly represent the molecular quadrupole that arises from charge separations in the phenyl ring. For comparison, in table III we show the classical quadrupole (normal to the plane of the ring) for benzene, calculated from OPLS-AA partial charges and from partial charges derived from Hartree-Fock calculations using a range of basis sets. The OPLS-AA result is closest to the experimental value of -2.5×10^{-39} C m^2. We note that the Hartree-Fock partial charges in table III are basis set dependent, and that the minimal basis set STO-3G calculations (which has been used to obtain partial charges for large mesogens in previous studies e.g. [3]) severely under-estimates Θzz.

TABLE I Atom types for me5NF and GG5Cl

Atom	*mass*	*Type*
C	12.01	C in carbonyl carbon
CA	12.01	C in Benzene
CT	12.01	C alkanes
CZ	12.01	C in cyano
F	19.00	Fluorine
HA	1.008	H in Benzene
HC	1.008	H alkanes
NZ	14.01	N in cyano
O	16.00	O in carbonyl
OS	16.00	O in ester

TABLE II Nonbonded Parameters

atom	*charge/e*	σ/Å	ϵ/*kJ mol*$^{-1}$
CT	0.000	3.50	0.276
HC	0.060	2.50	0.126
CA	−0.115	3.55	0.293
HA	0.115	2.42	0.126
F	−0.246	2.94	0.255
CZ	0.395	3.65	0.628
NZ	−0.430	3.20	0.711
C	0.700	3.75	0.439
O	−0.800	2.96	0.879
OS	−0.400	3.00	0.711

TABLE III Classical quadrupole moments Θ_{zz} for benzene (normal to the plane of the ring), calculated from partial atomic charges. Results are given for OPLS-AA partial charges and partial charges derived from Hartree Fock calculations with a range of basis sets. (Quantum mechanical values of Θ_{zz} have also been included in column 4. The other components of the quadrupole are obtained from $\Theta_{zz} = -2\Theta_{xx} = -2\Theta_{yy}$)

Type of charges	*partial charge /e*$^-$	$\Theta_{zz}/10^{-39}$ *C m*^{2} *(classical)*	$\Theta_{zz}/10^{-39}$ *C m*^{2} *(quantum)*
OPLS-AA	0.115	−2.28	–
HF/STO-3G	0.062906	−1.25	−6.16
HF/6–31+g	0.232051	−4.61	−3.06
HF/6–31+g(d,p)	0.167034	−3.32	−3.07

To the nonbonded parameters we add standard bond length and bond angle data from the AMBER/OPLS force fields [27,28,40] (tables IV and V), and determine missing bond angle and torsional angle information from X-ray data and *ab initio* quantum calculations. For the latter we have used Gaussian94 [42] and carried out restricted Hartree-Fock calculations at the RHF/6–31G* level. Good force field data was unavailable for the ester group in me5CN. Consequently, we initially carried out a full *ab initio* energy minimisation for the mesogenic fragment phenyl benzoate. The results for the *ab initio* angles (shown in table VI) are in good agreement with single crystal X-ray diffraction data for this molecule [43]. We then carried out bond angle distortions from the equilibrium geometry to determine the harmonic force constants K_θ for the angles θ_1-θ_4 shown in figure 2. The latter are in good agreement with the parameters used in the MMFF94 and MM3 force fields (table VI) though we stress that these force fields also use higher order terms to describe deviations from harmonicity.

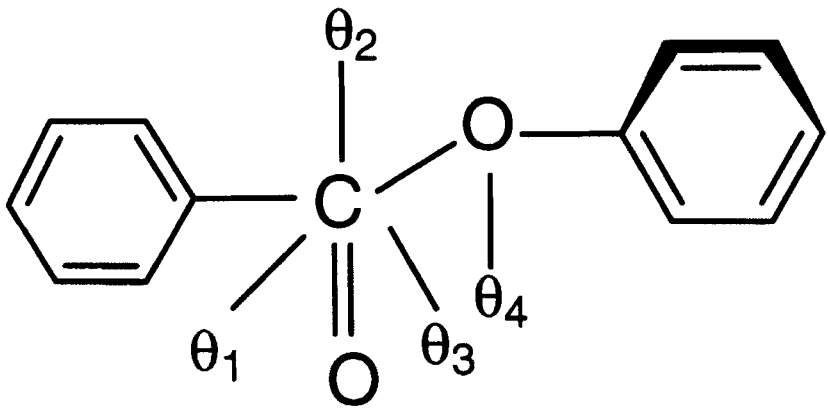

FIGURE 2 Definitions of bond angles θ_1, θ_2, θ_3, and θ_4 in phenyl benzoate

TABLE IV Bond lengths used

bond	*bond length/Å*
C – CA	1.490
C – C – O	1.229
CA – OS	1.364
C – OS	1.327
CA – CA	1.400
CA – CT	1.510

bond	*bond length/Å*
CA – NZ	1.261
CA – CZ	1.451
CZ – NZ	1.157
CT – CT	1.529
CT – HC	1.090
CA – F	1.354
CA – HA	1.080
CA – O	1.380
CT – OS	1.410
C – CT	1.522

TABLE V Bond angle parameters used

Angle	K_θ */kJ mol*$^{-1}$ *rad*$^{-2}$	*Angle /°*
CA – CA – CZ	292.88	120.0
CA – CZ – NZ	711.28	180.0
CA – CA – OS	292.88	120.0
CA – CA – F	334.72	113.0
C – CA – CA	355.64	120.0
C – CA – HA	146.44	120.0
CA – CA – CA	263.59	120.0
CA – CA – CT	292.88	120.0
CA – CA – HA	146.44	120.0
CA – CT – CT	263.59	114.0
CA – CT – HC	146.44	109.5
CT – CT – CT	244.35	112.7
CT – CT – HC	156.9	110.7
HC – CT – HC	138.07	107.8
OS – C – CA	338.90	111.4
C – OS – CT	347.27	116.9
HC – CT – OS	146.44	109.5
CT – C – O	334.72	120.4
C – CT – HC	146.44	109.5
OS – C – CT	338.90	111.4
O – O – C – CA	334.72	125.4
CA – OS – C	345.60	118.1
O – C – OS	347.27	123.4

TABLE VI Comparison of angle parameters for an ester group[a]

No	*crystal structure*	*ab initio*		*MM3*		*Merck*		*OPLS-AA*	
	θ/°	θ/°	K_θ	θ/°	K_θ	θ/°	K_θ	θ/°	K_θ
1	126.0	125.4	334.72	124.5	301.00	120.0	439.46	120.4	334.72
2	110.9	111.4	338.90	110.1	391.30	102.8	487.62	111.4	338.90
3	118.2	118.1	345.60	111.8	463.54	95.3	367.22	no	data
4	123.1	123.0	347.27	122 0	481.60	124.4	698.31	123.4	515.05

[a] force constants, K_θ, in kJ mol^{-1} rad^{-2}.

Some dihedral angle data for me5NF and GG5Cl are already available from the AMBER all-atom force field. The exception to this is the 3 dihedral angles in the linking ester group of me5NF and two inter-ring dihedrals for GG5Cl. In order to determine the unknown parameters for these five dihedral angles ($\phi_1 - \phi_5$), RHF/6–31G* calculations were performed on the mesogenic fragments, phenyl benzoate, phenyl acetate, methyl benzoate, 2-fluorobiphenyl and 2,2′-difluorobiphenyl which are shown in figure 3. However, using these data to obtain a set of torsional coefficients $\{V_i\}$ for each ϕ requires careful fitting. To do this we carried out a least squares fit to the *ab initio* data using the full molecular force field with the set of torsional coefficents $\{V_i\}$ used as variable parameters in the fit. At each step in the least squares minimisation we use the following procedure:

(i) start with the initial (approximate) values for $\{V_i\}$,

(ii) minimise the energy of the molecule in the force field for a set of values of the dihedral angle ϕ (with ϕ constrained at each point),

(iii) calculate the sum of the squares of the differences between the *ab initio* data and the data obtained from the energy minimisations.

In practise this procedure requires thousands of separate energy minimisation calculations to obtain converged values for $\{V_i\}$. However, it does ensure that all other force field contributions to the torsional angle energy (including the important contributions from nonbonded interactions) are taken properly into account in the fitting of $\{V_i\}$. All energy and least squares minimisations used Powell minimisation routines [44], and the final root mean square errors between fitted and *ab initio* data points were *0.47, 0.48, 1.37, 0.83, 0.96 kJ* mol^{-1} *for* ϕ_1-ϕ_5 respectively.

Results from the fitting procedure are shown in figures 4 and 5 and the calculated $\{V_i\}$ are included in table VII. The dihedral angle energy profiles for ϕ_1 and ϕ_3(figure 4) are symmetrical about 180° and were straight forward to fit requiring only a V_2 term in the Fourier expansion of equation 1. The minimum in the

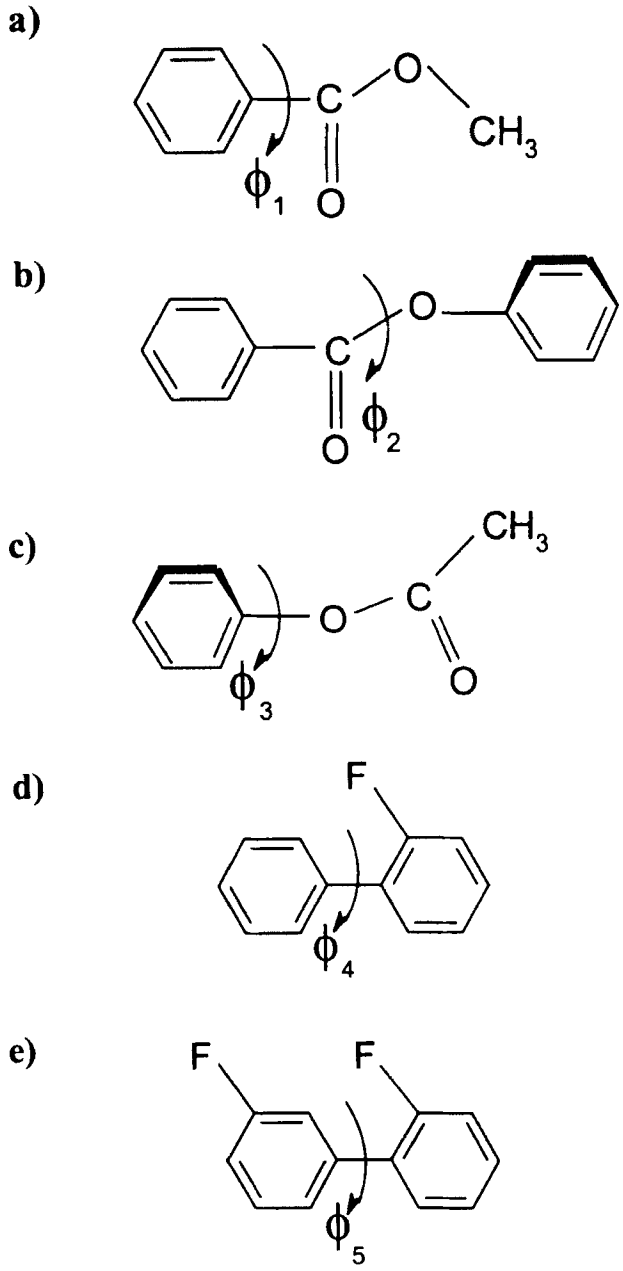

FIGURE 3 Structures of a) methyl benzoate, b) phenyl benzoate, c) phenyl acetate, d) 2-fluoro-biphenyl, and e) 2,2′-difluorobiphenyl and the definitions for the five dihedrals angles $\phi_1 - \phi_5$

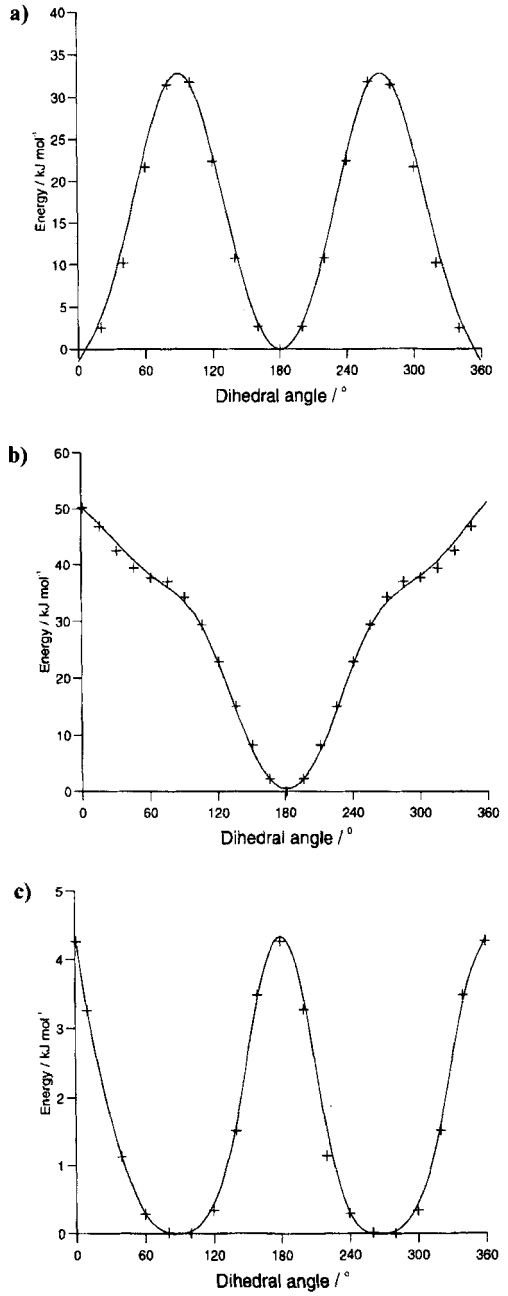

FIGURE 4 *Ab initio* (points) and fitted data (bold line) for torsional angles a) ϕ_1, b) ϕ_2, c) ϕ_3

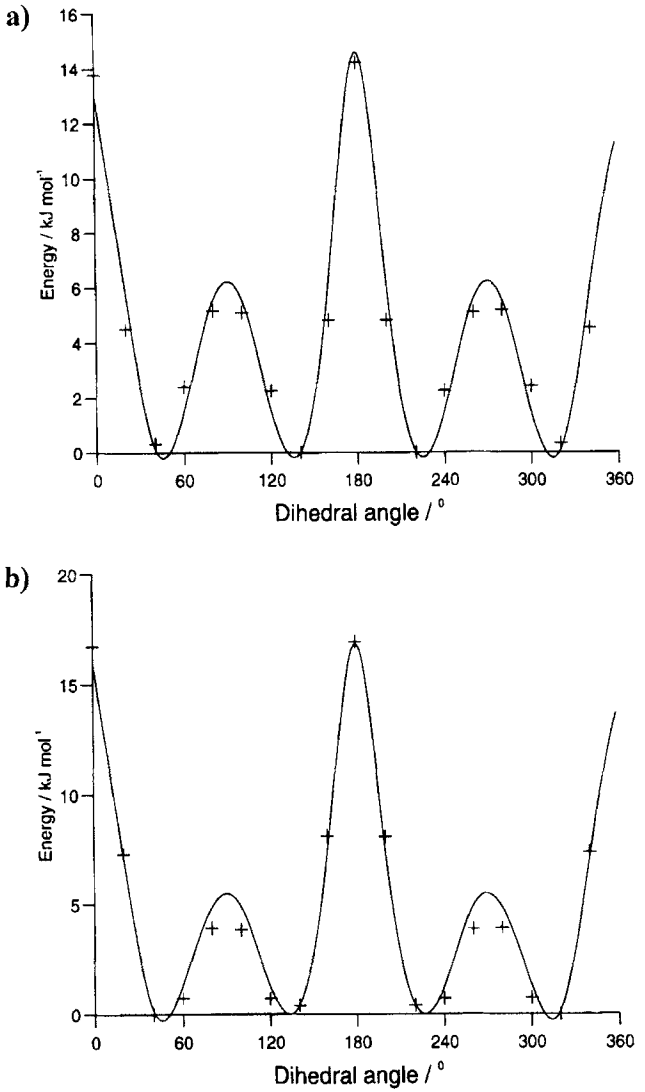

FIGURE 5 *Ab initio* (points) and fitted data (bold line) for torsional angles a) ϕ_4, b) ϕ_5

potential energy occurs at different dihedral angles: 180° (and 0°) for ϕ_1 and 0° for ϕ_3. This is in fairly good agreement with the X-ray single crystal structures for this molecule which gives ϕ_1 at 171.32° and ϕ_3 at 116.7°. However, we stress that when barriers to rotation are small, gas phase energy minima for dihedral angles often change slightly in the crystal in order to accomodate packing con-

straints. The barriers to rotation are given in table VIII. For comparison the *trans-gauche* conversion barriers in an alkyl chain are approximately 13.6 kJ mol^{-1} for a typical liquid crystal in the gas phase, calculated from plane-wave GGA DFT [45]. For ϕ_1, at room temperature (RT $\approx$ 2.5 kJ mol^{-1} at 298 K) we would therefore expect severely restricted rotation between two equally populated states but would expect almost free rotation for ϕ_3. The *ab initio* calculations for ϕ_2 (in phenyl benzoate) were significantly more expensive than for ϕ_1 and ϕ_3, and the fitting could only take place once values of $E(\phi_1)$ and $E(\phi_3)$ had been obtained. We obtain a good fit with V_1, V_2 and V_3 terms. Here we note that the barrier is extremely high (table VIII) and most of this contribution arises from the steric repulsions between the two phenyl groups that arises for rotations about ϕ_2. Finally, we note that the phenyl-ester-phenyl structure in phenyl benzoate is easy to prepare synthetically and so is commonly used as a linking group in calamitic liquid crystals. It is often assumed to be coplanar in its minimum energy conformation. This is not the case in the crystal structure or in this work. However, the coplanar configuration is only 4.6 kJ mol^{-1} higher in energy than the minimum energy configuration and so is easily accessible. The effective torsional barrier measured in a liquid crystal phase will always contain a contribution that arises from the preferred packing arrangement of molecules in the bulk. Depending on the phase, this has been seen to influence conformational energies by 2–3 kJ mol^{-1} [46]. It will be interesting to see if local packing of molecules in an orientationally ordered phase preferentially selects a planar arrangement of molecules in contrast to the gas phase. However, this must await simulations of a bulk liquid crystal phase with this force field.

TABLE VII Torsional Parameters in kJ mol^{-1}

dihedral angle	V_1	V_2	V_3	V_4	V_6
HC – CT – CT – HC	0.000	0.000	1.331		
HC – CT – CT – CT	0.000	0.000	1.531		
CT – CT – CT – CT	7.280	–0.657	1.167		
HC – CT – CA – CA	0.000	0.000	0.000		
CT – CT – CA – CA	0.000	0.000	0.000		
HC – CT – CT – CA	0.000	0.000	1.933		
CA – CA – CA – CA	0.000	39.748	0.000		
CA – CA – CA – HA	0.000	39.748	0.000		
HA – CA – CA – HA	0.000	39.748	0.000		
OS – C – CA – CA	0.000	11.171	0.000		
CA – C – OS – CA	10.862	17.016	0.916		

dihedral angle	V_1	V_2	V_3	V_4	V_6
O – C – OS – CA	10.862	17.016	0.916		
C – OS – CA – CA	0.000	7.950	0.000		
O – C – CA – CA	0.0 00	8.996	0.000		
CA – CA – CA – CA(F)	–0.142	6.284	–0.201		
CA(F) – CA – CA – CA(F)	0.791	9.305	0.000	4.322	2.594

ϕ_4 was fitted with three Fourier terms V_1, V_2 and V_3, but surprisingly the torsional angle ϕ_5 required a minimum of five Fourier coefficients V_1, V_2, V_3, V_4, and V_6 to achieve the same quality of fit. In table VIII we have also included molecular mechanics dihedral barrier results using the augmented form of the MM3 force field available in the CAChe modelling suite [47] to calculate energy barriers. The MM3/CAChe results consistently over-estimate the *ab initio* energy barriers apart from the lower of the two energy barriers in the dihedrals ϕ_4 and ϕ_5, which are underestimated. In some cases (ϕ_1, ϕ_2) the MM3/CAChe results are extremely poor. While this may not be significant for minimum energy configurations, the energy barriers are of major importance in a molecular dynamics calculation.

TABLE VIII Comparison of *ab initio*, LCFF and MM3 torsional energy barriers. Values given are in kJ mol^{-1}

dihedral	*ab initio energy barriers*	*LCFF energy barriers*	*MM3*
ϕ_1	31.8	32.8	106.1
ϕ_2	49.7	50.2	68.9
ϕ_3	4.6	4.3	8.4
ϕ_4	14.2, 5.9	15.1, 6.1	37.0, 1.2
ϕ_5	18.9, 5.6	19.4, 5.7	16.9, 0.8

4 BULK SIMULATIONS

The LCFF was tested by computing the structures and liquid state densities of the fragment molecules phenyl acetate, methyl benzoate, and the mesogens me5NF and GG5Cl. In each case an initial molecular configuration was generated from a *bcc* lattice in which 216 molecules were given a small random displacement from their lattice positions and randomly orientated inside a cuboidal simulation box at gas phase densities. Initially, the isothermal-isobaric algorithm of Berendsen was employed to relax the molecular configuration. We used a nominal pres-

sure of 10^5 Pa until the desired density of approximately 1 g cm^{-3} was achieved. Thereafter the system was equilibrated using a Nosé-Hoover thermostat and a Hoover barostat at a pressure of 1 atmosphere, employing relaxation times of 1 ps and 4 ps respectively. The simulations retained cubic periodic boundary conditions throughout, employed the Verlet leap frog algorithm with a time-step of 2 fs and made use of the SHAKE procedure [36] to constrain bond lengths. However, other than this the molecules are treated as fully flexible, allowing for angle bending and dihedral angle changes. The *long-range* electrostatic interactions were handled by an Ewald sum with the convergence parameter α set at 0.48 $Å^{-1}$ and 6 k-vectors were used for each of the directions (x,y,z) in the periodic box. A cut-off of 9 Å was used for the *short range* 12:6 interactions. All calculations used the DL_POLY_2.11 program [48]. A typical run consisted of a equilibration period of (in total) 1000 ps, folllowed by a production run of 500 ps.

Values of the mean density $\langle\rho\rangle$ were calculated throughout the simulations and the mean values at equilibrium are given in table IX. $\langle\rho\rangle$ values are in excellent agreement with experiment (better than 1%) for the three systems with available experimental data at the corresponding simulation temperatures. For GG5Cl experimental density data is not available in the isotropic phase. However, a value of $\rho = 1.158$ g cm^{-3} is available in the nematic phase at 338 K (2 K above the freezing point and 53.8 K below the clearing point). Given that this temperature is 60 K below our simulation temperature, our computed density for GG5Cl is in the range that we would predict based on typical density changes across the nematic/isotropic temperature range. Small errors in Lennard-Jones ε or σ parameters can lead to large variations in the density, so our results give us a high degree of confidence in the nonbonded parameters in the force field. Moreover, significant deviations from the correct liquid state torsional potentials influence the local packing arrangements of molecules: again leading to poor predictions for the density. Following the procedure of Jorgensen and co-workers [24], we have calculated also the heat of vaporization for phenyl acetate and methyl benzoate at 298 K. The results of 10.60 kJ mol^{-1} for phenyl acetate and 13.31 kJ mol^{-1} for methyl benzoate, again compare well with the experimental values of 10.32 kJ mol^{-1} [49] and 13.20 kJ mol^{-1} [50].

TABLE IX Computed and experimental densities

liquid	*T / K*	$\langle\rho\rangle$/g cm^{-3}	ρ *(exp)*/g cm^{-3}
me5NF	303	1.1126	1.1300
GG5Cl	393	1.068	–
phenyl acetate	298	1.0818	1.0780
methyl benzoate	298	1.9011	1.0838

5 CONCLUSIONS

The current study describes preliminary work in the development and testing of a new force field designed specifically for liquid crystal molecules. We list force field parameters suitable for the mesogens me5NF and GG5Cl that contain many of the key structural elements found in many calamitic liquid crystals: conjugated phenyl rings, lateral fluorination, an ester group, alkyl chains, terminal chloro and cyano groups. The force field builds upon the existing all-atom AMBER and OPLS force fields, with new angle and torsional energy parameters derived from fitting to *ab initio* RHF/6–31G* molecular orbital calculations. The force fields have been tested on liquid state simulations of the molecules phenyl acetate and methyl benzoate and the mesogens me5NF and GG5Cl. We find good agreement between the simulations results and experimental densities and heats of vaporization (where available). The force fields for me5NF and GG5Cl are used in the following paper to study dipole correlation in the pretransitional region of the isotropic phase.

Acknowledgements

The authors wish to thank the University of Durham IT service for providing computer time on its parallel Silicon Graphics system, and the UK EPSRC for providing computer time on a Cray T3E. MJC wishes to thank the EPSRC and Merck UK Ltd. for providing a research studentship (1997–2000), and Merck UK Ltd (Southampton) for the gift of a DEC 433 a.u. workstation. The authors wish to thank Dr. M. Bremer and Dr. M. Heckmeier (Merck KGaA, Darmstadt) for valuable discussions and for supplying experimental data for me5CN and GG5Cl.

References

[1] Wilson, M. R. In *Handbook of Liquid Crystals*, Demus, D., Goodby, J., Gray, G. W., Spiess, H.-W., and Vill, V., editors, volume 1, chapter III.3. Wiley-VCH, Weinheim (1998).
[2] Wilson, M. R. In *Structure and Bonding: Liquid Crystals*, Mingos, M., editor. Springer-Verlag, Heidelberg (1999).
[3] Wilson, M. R. and Allen, M. P. *Molec. Cryst. Liq. Cryst.* **198**, 465 (1991).
[4] Wilson, M. R. and Allen, M. P. *Liq. Cryst.* **12**, 157 (1992).
[5] Wilson, M. R. *J. Molec. Liq.* **68**, 23 (1996).
[6] Ono, I. and Kondo, S. *Molec. Cryst. Liq. Cryst.* **8**, 69 (1991).
[7] Krömer, G., Paschek, D., and Geiger, A. *Ber. Bunsenges Phys. Chem.* **97**, 1188 (1993).
[8] Huth, J., Mosell, T., Nicklas, K., Sariban, A., and Brickmann, J. *J. Phys. Chem.* **98**, 768 (1994).
[9] Cross, C. W. and Fung, B. *J. Chem. Phys.* **101**, 6839 (1994).
[10] Kolmolkin, A. V., Laaksonen, A., and Maliniak, A. *J. Chem. Phys.* **101**, 4103 (1994).
[11] McBride, C., Wilson, M. R., and Howard, J. A. K. *Molec. Phys.* **93**, 955 (1998).
[12] B. R. Gelin, M. K. *Biochemistry* **18**, 1256 (1979).
[13] Brooks, B. R., Bruccoleri, R. E., Olafson, B. D., States, D. J., Swaminathan, S., and Karplus, M. *J. Comput. Chem.* **4**, 187 (1983).

[14] Weiner, S.J., Kollman, P. A., Case, D. A., Singh, U. C., Ghio, C., Alagona, G., Profeta, S., and Weiner, P. *J. Am. Chem. Soc.* **106**, 765 (1984).
[15] Cornell, W. D., Cieplak, P., Bayly, C. I., Gould, I. R., Merz, K. M. (Jr.), Ferguson, D. M., Spellmeyer, D. C., Fox, T., Caldwell, J. W., and Kollman, P. A. *J. Am. Chem. Soc.* **117**, 5179 (1995).
[16] Allinger, N. L., Tribble, M. T., Miller, M. A., and Wertz, D. H. *J. Am. Chem. Soc.* **93**, 1637 (1971).
[17] Allinger, N. L. *J. Am. Chem. Soc.* **99**, 8127 (1977).
[18] Allinger, N. L., Yuh, Y. H., and Lii, J. *J. Am. Chem. Soc.* **111**, 8551 (1989).
[19] Allinger, N. L., Chen, K. S., and Lii, J. H. *J. Comput. Chem.* **17**, 642 (1996).
[20] Nevins, N., Chen, K. S., and Allinger, N. L. *J. Comput. Chem.* **17**, 669 (1996).
[21] Nevins, N., Lii, J. H., and Allinger, N. L. *J. Comput. Chem.* **17**, 695 (1996).
[22] Nevins, N. and Allinger, N. L. *J. Comput. Chem.* **17**, 730 (1996).
[23] Allinger, N. L., Chen, K. S., J. A. Katzenellenbogen, and S. R. Wilson, G. M. A. *J. Comput. Chem.* **17**, 747 (1996).
[24] Jorgensen, W. L., Madura, J. D., and Swenson, C. J. *J. Am. Chem. Soc.* **106**, 6638 (1984).
[25] Jorgensen, W. L. and Swensen, C. J. *J. Am. Chem. Soc.* **107**, 569 (1985).
[26] Jorgensen, W. L. and Swensen, C. J. *J. Am. Chem. Soc.* **107**, 1489 (1985).
[27] Jorgensen, W. L., Maxwell, D. S., and Tirado-Rives, J. *J. Am. Chem. Soc.* **118**, 11225 (1996).
[28] Jorgensen, W. L., Maxwell, D. S., and Tirado-Rives, J. *Support material from J. Am. Chem. Soc.* **118**, 11225 (1996).
[29] Cook, M. J. and Wilson, M. R. *Molec. Cryst. Liq. Cryst.*, in press (2001).
[30] Halgren, T. A. *J. Comput. Chem.* **17**, 490 (1996).
[31] Halgren, T. A. *J. Comput. Chem.* **17**, 520 (1996).
[32] Halgren, T. A. *J. Comput. Chem.* **17**, 553 (1996).
[33] Halgren, T. A. and Nachbar, R. B. *J. Comput. Chem.* **17**, 587 (1996).
[34] Halgren, T. A. *J. Comput. Chem.* **17**, 616 (1996).
[35] Kaminski, G. and Jorgensen, W. L. *J. Phys. Chem.* **100**, 18010 (1996).
[36] Ryckaert, J. P., Ciccotti, G., and Berendsen, H. J. C. *J. Chem. Phys.* **23**, 327 (1977).
[37] Wilson, M. R. *J. Chem. Phys.* **107**, 8654 (1997).
[38] Cook, M. J. and Wilson, M. R. *Liq. Cryst.*, accepted for publication (2000).
[39] Garcia, E., Glaser, M. A., Clark, N. A., and Walba, D. M. Theochem – *J. Molec. Struc.* **464**, 39 (1999).
[40] Jorgensen, W. L. and Nguyen, T. B. *J. Comput. Chem.* **14**, 195 (1993).
[41] Jorgensen, W. L. and Tirado-Rives, J. *J. Am. Chem. Soc.* **110**, 411 (1988).
[42] Gaussian 94 is a package written by M. J. Frisch and A. Frisch and J. B. Foresman, copyright Gaussian, Inc., Carnegie office park, Pittsburgh, (1994–1996).
[43] Shibakami, M. and Sekiya, A. *Acta Crystallogr. Sect C* **51**, 326 (1995).
[44] Press, W. H., Flannery, B.P., A. Teukolsky, S., and Vetterling, W. T. *Numerical Recipies*, chapter 10. Cambridge University Press (1988).
[45] Cheung, D. A., Wilson, M. R., and Clark, S.J., unpublished work.
[46] Wilson, M. R. *J. Chem. Phys.* **107**, 8654 (1997).
[47] *CAChe Satellite: A Chemists Guide to CAChe for Windows.* Oxford Molecular Group Inc., (1995).
[48] Forester, T. R. and Smith, W. *DL_POLY_2.11*. DL_POLY is a package of molecular simulation routines written by W. Smith and T. R. Forester, copyright The Council for the Central Laboratory of the Research Councils, Daresbury Laboratory at Daresbury, Nr. Warrington (1996).
[49] Lebedeva, N. D. and Katin, Y. A. *Russ. J. Phys. Chem.* **46**, 1088 (1972).
[50] Lide, D. R. and Kehiaian, H. V. *CRC Handbook of Thermophysical and Thermochemical data.* CRC Press, (1994).